Mesoscopic Modeling in the Kinetic Theory of Adsorbates

ARTICLE *in* THE JOURNAL OF PHYSICAL CHEMISTRY · DECEMBER 1996

Impact Factor: 2.78 · DOI: 10.1021/jp961668w

2 AUTHORS, INCLUDING:

Alexander S. Mikhailov
Fritz Haber Institute of the Max Planck Society
285 PUBLICATIONS **6,217** CITATIONS

Mesoscopic Modeling in the Kinetic Theory of Adsorbates

M. Hildebrand and A. S. Mikhailov*

Abteilung Physikalische Chemie, Fritz-Haber-Institut der Max-Planck-Gesellschaft, Faradayweg 4-6, 14195 Berlin (Dahlem), Germany

Received: June 6, 1996[⊗]

A mesoscopic description of surface chemical reactions, aimed to provide a link between microscopic lattice models and reaction−diffusion equations, is formulated. Such a description is needed when large populations of nanoscale structures are considered or patterns characterized by a combination of macroscopic and microscopic lengths are investigated. By using the example of an adsorbate with attractive lateral interactions between molecules, the mesoscopic evolution equation for fluctuating coverages is derived from the microscopic master equation of the respective kinetic lattice model. This stochastic equation is applied to study phenomena of pattern formation related to adsorbate phase transitions.

1. Introduction

Development of experimental methods, such as field ion microscopy or scanning tunneling microscopy, has opened up the possibility to monitor chemical reactions on the surfaces of metal catalysts in real time with an almost atomic resolution. As a consequence of this, microscopic reaction properties, which could previously have been only deduced through their influence on global reaction rates or other macroscopic properties of a reaction, become directly observable. Experiments have shown that the adsorbate molecules often form fluctuating clusters or islands.[1] In the presence of reactions, nonequilibrium spatiotemporal structures with sizes lying in the nanometer range have been observed.[2]

An important role in determining the process of pattern formation at nanoscales on metal surfaces is played by interactions between the adsorbed molecules. These interactions are usually classified into direct (van der Waals, electrostatic, bond formation) and indirect, substrate-mediated interactions.[3] The indirect attractive or repulsive interactions are mainly explained by local changes of the surface electronic wave functions which are induced by adsorbed molecules and usually have a radius of several lattice lengths.[4,5] The presence of an adsorbate can also modify the local crystallographic structure of the substrate's surface layer and thus produce deformations and stresses in the crystal. This effect leads to long-range indirect elastic interactions between adsorbed molecules and their clusters.[6−8]

Because of significant interactions between the molecules within a monolayer, the adsorbates can be viewed as condensed systems or "soft matter".[9] However, in contrast to other examples of soft condensed systems, such as wetting liquid films[10] or Langmuir−Blodgett films,[11] the molecules forming a reactive adsorbate participate in chemical reactions.

Catalytic surface reactions are fast and may be diffusion-controlled. However, in contrast to diffusion-controlled reactions in weak solutions, reacting adsorbate molecules do not represent a small subsystem inside a solvent. Instead, they constitute the bulk of a condensed system. Hence, fast chemical reactions in the adsorbates can directly compete with potential interactions between the molecules. Together, they determine the physical properties of an adsorbate and the kinds of spatiotemporal patterns formed by it.

Two different theoretical approaches are presently used to describe spatiotemporal pattern formation in catalytic surface reactions. The approach based on reaction-diffusion models (see ref 12) neglects potential interactions between the reacting molecules and essentially treats an adsorbate like a two-dimensional "ideal gas" whose molecules perform random diffusional motion. Only to some extent these interactions could later be phenomenologically taken into account by assuming the coverage dependence of diffusion coefficients or desorption rates.

The reaction-diffusion models provide a relatively good description of spatiotemporal patterns, such as propagating excitation waves, spirals, or oscillatory cellular structures, with wavelengths ranging from a few micrometers to several hundreds of micrometers.[13−15] However, they meet difficulties when nanoscale structures (i.e. reactive islands or sharp propagating fronts) must be described. The sizes of these structures are already smaller than the diffusion length, representing the minimal characteristic length in any reaction-diffusion model.

Note that even when macroscopic reaction properties, such as the reaction rate, are considered, they may still be significantly influenced by the collective behavior of large populations of nanoscale structures, and therefore a microscopic description is needed. For instance, it was recently shown that the lifetime of the nanoscale reactive islands can be responsible for chaotic oscillations of the reaction rate in catalytic surface reactions.[16]

Microscopic lattice models take explicitly into account the random motion of individual molecules and reactions between them.[17−19] Such models are used in Monte Carlo simulations that yield valuable information about the microscopic reaction properties.[20,21] However, memory and speed of available computers limit the maximal spatial size of the modeled system, and therefore systematic simulations of nanoscale or submicrometer structures and their populations are difficult. Analytical methods, such as the mean-field or Kirkwood approximations, describe statistical properties of uniform steady states.[22,23] They, however, are not suited for the description of individual patterns, such as moving interfaces or growing nuclei of a new phase.

Thus, there is a gap between the "macroscopic" reaction-diffusion theory, yielding description of waves and spatial structures but not taking into account fluctuations and interac-

[⊗] Abstract published in *Advance ACS Abstracts,* November 1, 1996.

S0022-3654(96)01668-1 CCC: $12.00

tions between the particles, and the microscopic lattice theory that primarily addresses the statistical properties of fluctuations. To bridge these two approaches, a mesoscopic description is desirable.

Similar to reaction-diffusion models, this mesoscopic description should be formulated in terms of adsorbate coverages. However, the mesoscopic evolution equation for the coverages would be stochastic and would include internal noises. The form and intensity of these noises would be determined from the analysis of the master equation of the underlying lattice model.

Mesoscopic modeling has previously been developed for the description of other reaction−diffusion systems, if fluctuations due to reactions and diffusion have been significant.[24−27] To apply such methods in studies of monomolecular adsorbates, the finite occupancy of lattice sites and the existence of potential interactions between adsorbate molecules should be taken into account.

To illustrate the principles of the mesoscopic description of adsorbates and analyze its general properties, we consider below a simple example of an adsorbate formed by a single kind of molecule with strong attractive lateral interactions between them. This system undergoes a phase transition leading to two different adsorbate phases characterized by low (dilute phase) and high (dense phase) coverages.

The formulation and general discussion of the mesoscopic evolution equation for this problem are given in the next section. The third section deals with the properties of the deterministic limit of this equation. Attention is focused here on the properties of moving interfaces that separate regions with two different adsorbate phases. In the fourth section we consider the effects of fluctuations and show that the model allows simulation of the process of stochastic nucleation at the first-order phase transition. Appendix A contains the derivation of the mesoscopic evolution equation from the respective microscopic lattice model. Appendix B is devoted to the discussion of some thermodynamic properties of the considered phase transition.

2. Mesoscopic Description of Adsorbates

We start from the microscopic lattice model. Suppose that molecules of an adsorbate may occupy only the sites of a certain planar lattice with μ lattice sites per unit area. Multiple occupation of the sites is forbidden. A molecule can arrive at a site either from the gas phase or from neighboring sites of the lattice. Under the simplest assumptions, the adsorption rate, i.e. the probability of the arrival of a molecule from the gas phase at a given vacant site of the lattice, is $w_a = k_a p$, where k_a is the sticking coefficient and p is the (constant) partial pressure in the gas phase.

The desorption rate, i.e. the probability per unit time that a molecule leaves its site $\mathbf{R}$ and goes into the gas phase, is

$$w_d = k_{d,0} \exp\left(\frac{U(\mathbf{R})}{k_B T}\right) \tag{1}$$

where $k_{d,0}$ is the desorption rate for a molecule occupying an isolated site and $U(\mathbf{R})$ is the potential induced at a given site by interactions with other adsorbate molecules; T is the temperature and k_B is the Boltzmann constant.

A molecule can jump from a site $\mathbf{R}$ to a neighboring vacant site $\mathbf{R}_1$ in the lattice with the probability $w(\mathbf{R},\mathbf{R}_1)$ per unit time which is determined according to the Metropolis algorithm, i.e.

$$w(\mathbf{R},\mathbf{R}_1) = \begin{cases} \nu_0, & \text{if } \Delta E < 0 \\ \nu_0 \exp\left(-\dfrac{\Delta E}{k_B T}\right), & \text{if } \Delta E > 0 \end{cases} \tag{2}$$

where $\Delta E = U(\mathbf{R}_1) - U(\mathbf{R})$ and ν_0 is the hopping rate of a particle in absence of interactions.

The potential $U(\mathbf{R})$ experienced by a molecule at a given site $\mathbf{R}$ is given by

$$U(\mathbf{R}) = -\sum_{\mathbf{R}'} u(\mathbf{R}-\mathbf{R}')\, n(\mathbf{R}') \tag{3}$$

where $n(\mathbf{R}')$ is the occupation number at site $\mathbf{R}'$, i.e. $n = 1$ for an occupied site and $n = 0$ otherwise. The function $u(\mathbf{r})$ represents the binary potential of attractive interaction between two adsorbate molecules that are separated by a distance $\mathbf{r}$ on the surface; for convenience we have introduced the minus sign in eq 3, so that the function u is positive in this case. The summation in eq 3 is performed over all lattice sites $\mathbf{R}'$, but because the function $u(\mathbf{r})$ vanishes for the distances exceeding the interaction radius, it is actually reduced to a summation over a certain neighborhood of the site $\mathbf{R}$.

Using the above assumptions, a microscopic master equation for the joint probability distribution $P(\{n(\mathbf{R})\},t)$ can be written. It has the form

$$\begin{aligned} \frac{\mathrm{d}}{\mathrm{d}t}P = \sum_{\mathbf{R}} k_a p\{n(\mathbf{R})P(/n(\mathbf{R})-\mathbf{1}/) - (1 - n(\mathbf{R}))P\} + \\ \sum_{\mathbf{R}} k_{d,0} \exp\left[-\frac{1}{k_B T}\sum_{\mathbf{R}'} u(\mathbf{R}-\mathbf{R}')\, n(\mathbf{R}')\right] \times \\ \{(1 - n(\mathbf{R}))P(/n(\mathbf{R})+1/) - n(\mathbf{R})P\} + \\ \sum_{\mathbf{R},\mathbf{R}_1} w(\mathbf{R}_1,\mathbf{R})\{n(\mathbf{R})(1 - n(\mathbf{R}_1))P(/n(\mathbf{R})-1,n(\mathbf{R}_1)+1/) - \\ (1 - n(\mathbf{R}))n(\mathbf{R}_1)P\} \end{aligned} \tag{4}$$

where

$$\begin{aligned} w(\mathbf{R},\mathbf{R}_1) = \nu_0 \exp\left\{-\frac{1}{k_B T}H\left[\sum_{\mathbf{R}'}(u(\mathbf{R}-\mathbf{R}') - \right.\right. \\ \left.\left. u(\mathbf{R}_1-\mathbf{R}'))n(\mathbf{R}')\right]\sum_{\mathbf{R}'}(u(\mathbf{R}-\mathbf{R}') - u(\mathbf{R}_1-\mathbf{R}'))n(\mathbf{R}')\right\} \end{aligned} \tag{4a}$$

The summation over $\mathbf{R}_1$ includes only the sites that represent nearest neighbors of the site $\mathbf{R}$; the step function $H(z)$ is defined as $H(z) = 1$ for $z > 0$ and $H(z) = 0$ for $z \le 0$. We use short notations $P(/n(\mathbf{R})\pm 1/)$ which mean that the set of occupation numbers in this distribution differs from that in the distribution P only at the site $\mathbf{R}$ where the occupation number $n(\mathbf{R})$ is decreased (increased) by one.

The microscopic master equation (eq 4) is complicated and, apart from direct numerical integration, can be studied only under certain approximations. For instance, one may use this equation to derive a system of coupled equations for the correlation functions $\langle n(\mathbf{R})\, n(\mathbf{R}')...n(\mathbf{R}^{(k)})\rangle$ of various orders k and, by assuming the statistical uniformity of the system and applying the mean-field or the Kirkwood approximations, truncate this system, thus arriving at the equations for the mean densities and binary correlation functions.

Our approach is different. We introduce coarse graining by dividing the lattice into a set of boxes, each containing a large number of sites. This allows us to define the local coverage $c(\mathbf{r},t)$ as the number of adsorbate particles inside a box divided by the number of sites inside it. This coverage is still subject to random variations.

The principal assumption is that, inside each box, complete mixing occurs, and therefore the state of the system is already specified if the numbers of particles in all boxes are known. When interactions between the particles are present, the size of a box should be smaller than the interaction radius. Since the box still contains a large number of lattice sites, the interaction radius must be relatively large.

As noted above, the attractive substrate-mediated interactions in the adsorbates usually extend only over a few lattice lengths. Though the mesoscopic theory is not fully justified here and cannot replace Monte Carlo simulations of the respective microscopic lattice models, it may still be used for the qualitative interpretation of experimental and computational data. Moreover, though we do not specifically consider such a situation, the theory would also be applicable in the case of long-range interactions induced by elastic deformations in the substrate (such interactions are, however, usually repulsive). Below the interaction radius is assumed to be sufficiently large to validate the mesoscopic approach.

In Appendix A we show how, proceeding from the microscopic master equation 4, a mesoscopic evolution equation for the fluctuating local coverage can be derived. The basic steps of this derivation are that first the master equation is written in the coarse-grained approximation, i.e. for the numbers of particles inside the boxes. When such numbers are large, the local coverage, defined as the fraction of occupied sites inside a box, does not significantly change as a result of an individual event of adsorption, desorption, or diffusion processes. By performing an expansion in powers of the inverse number of sites inside a box and introducing continuous spatial coordinates, we arrive at a functional Fokker−Planck equation for the probability distribution $P([c(\mathbf{r})],t)$. After that, by applying the methods of the theory of random processes, we find the corresponding stochastic partial differential equation for the fluctuating field $c(\mathbf{r},t)$.

The mesoscopic evolution equation for the local fluctuating coverage $c(\mathbf{r},t)$ is

$$\frac{\partial c}{\partial t} = k_a p(1-c) - k_{d,0}\exp\left(\frac{U(\mathbf{r})}{k_B T}\right)c + \frac{\partial}{\partial \mathbf{r}}\left\{\frac{D}{k_B T}(1-c)c\frac{\partial U}{\partial \mathbf{r}}\right\} + D\frac{\partial^2 c}{\partial \mathbf{r}^2} + \frac{1}{\mu^{1/2}}[k_a p(1-c)]^{1/2} f_a(\mathbf{r},t) + \frac{1}{\mu^{1/2}}[k_{d,0}c]^{1/2}\exp\left(\frac{U(\mathbf{r})}{2k_B T}\right) f_d(\mathbf{r},t) + \frac{1}{\mu^{1/2}}\frac{\partial}{\partial \mathbf{r}}\{[2Dc(1-c)]^{1/2}\mathbf{f}(\mathbf{r},t)\} \quad (5)$$

The potential U is given by

$$U(\mathbf{r}) = -\int u(\mathbf{r}-\mathbf{r}')\, c(\mathbf{r}')\, d\mathbf{r}' \quad (6)$$

and $f_a(\mathbf{r},t)$, $f_d(\mathbf{r},t)$, and $\mathbf{f}(\mathbf{r},t)$ are independent white noises of unit intensity

$$\langle f_a(\mathbf{r},t)\, f_a(\mathbf{r}',t')\rangle = \delta(\mathbf{r}-\mathbf{r}')\,\delta(t-t'), \quad \langle f_d(\mathbf{r},t)\, f_d(\mathbf{r}',t')\rangle = \delta(\mathbf{r}-\mathbf{r}')\,\delta(t-t')$$

$$\langle f^{(\alpha)}(\mathbf{r},t)\, f^{(\beta)}(\mathbf{r}',t')\rangle = \delta_{\alpha\beta}\delta(\mathbf{r}-\mathbf{r}')\,\delta(t-t'), \quad \alpha,\beta = 1,2 \quad (7)$$

The diffusion constant is $D = \nu_0 a^2$ where a is the lattice length; other parameters have the same meaning as in the microscopic master equation 3. The stochastic partial differential equation 5 should be interpreted in the Ito sense. The last three terms on the right side of eq 5 represent *internal noises* of the adsorption, desorption, and diffusion processes. In the next section we first analyze the properties of this equation in the macroscopic limit, i.e. when such noises can be neglected.

3. The Macroscopic Limit

Neglecting the noise terms in the stochastic partial differential equation 6, we arrive at the deterministic integrodifferential equation for the coverage in the presence of attractive lateral interactions between the adsorbed molecules (this equation has earlier been phenomenologically constructed in ref 28)

$$\frac{\partial c}{\partial t} = k_a p(1-c) - k_{d,0}\exp\left\{-\frac{1}{k_B T}\int u(\mathbf{r}-\mathbf{r}')\, c(\mathbf{r}')\, d\mathbf{r}'\right\}c - \frac{\partial}{\partial \mathbf{r}}\left\{\frac{D}{k_B T}(1-c)c\frac{\partial}{\partial \mathbf{r}}\int u(\mathbf{r}-\mathbf{r}')\, c(\mathbf{r}')\, d\mathbf{r}'\right\} + D\frac{\partial^2 c}{\partial \mathbf{r}^2} \quad (8)$$

The first two terms in this equation describe adsorption and desorption of particles; the desorption rate constant depends on the local coverage because of the attractive interactions between the molecules.

The third term describes the viscous surface flow of the adsorbate in the presence of the force given by the gradient of the local potential. Since the flow can pass only through vacant sites this term contains the factor $1 - c$. According to Einstein's relationship, the coefficient $D/k_B T$ gives the surface mobility of the adsorbate particles.

The last term accounts for the diffusion of particles. The diffusion coefficient D in this equation, as follows from its derivation on the basis of the microscopic master equation, represents the surface diffusion constant for an individual particle, in absence of other adsorbate particles. Note that, although particles can move only to vacant sites, this does not influence the form of the diffusion term (however, as shown in Appendix A, the internal noise due to diffusion is affected by this).

Equation 8 can be applied to describe macroscopic phenomena of pattern formation in the presence of attractive interactions between the particles in the adsorbate. When the interaction radius is small as compared to the diffusion length, this equation can be simplified.

If the coverage c does not significantly vary within the interaction radius, we can use the approximation

$$\int u(\mathbf{r}-\mathbf{r}')\, c(\mathbf{r}')\, d\mathbf{r}' \approx \int u(\mathbf{r}-\mathbf{r}')\left[c(\mathbf{r}) + (\mathbf{r}'-\mathbf{r})\frac{\partial c}{\partial \mathbf{r}} + \frac{1}{2}(\mathbf{r}'-\mathbf{r})^2\frac{\partial^2 c}{\partial \mathbf{r}^2} + ...\right]d\mathbf{r}' \quad (9)$$

where the spatial derivatives are taken at point $\mathbf{r}$. Therefore, we have

$$\int u(\mathbf{r}-\mathbf{r}')\, c(\mathbf{r}')\, d\mathbf{r}' \approx u_0 c + \chi\frac{\partial^2 c}{\partial \mathbf{r}^2} \quad (10)$$

where the coefficients are

$$u_0 = \int u(\mathbf{r})\, d\mathbf{r} \quad (11)$$

$$\chi = \frac{1}{2}\int r^2 u(\mathbf{r})\, d\mathbf{r} \quad (12)$$

and we have taken into account that, by symmetry considerations

$$\int \mathbf{r}u(\mathbf{r})\, d\mathbf{r} = 0 \quad (13)$$

Note that if the binary interaction potential $u(\mathbf{r})$ has the maximal intensity $u(0) = u_{max}$ and the characteristic radius r_0, the coefficients in eq 10 can be estimated by an order of magnitude as $u_0 \approx u_{max} r_0^2$ and $\chi \approx u_{max} r_0^4$, and therefore, $\chi \approx u_0 r_0^2$.

Under the condition that the expansion 9 is valid, the term with the second derivative in eq 10 is small in comparison with the first term in this equation. However, it should be retained in eq 8 because otherwise this equation can lead to divergencies. Substitution of eq 10 into eq 8 yields

$$\frac{\partial c}{\partial t} = k_a p(1-c) - k_{d,0} \exp\left\{-\frac{1}{k_B T}\left(u_0 c + \chi \frac{\partial^2 c}{\partial \mathbf{r}^2}\right)\right\} c + \frac{\partial}{\partial \mathbf{r}}\left\{D\left[1 - \frac{u_0}{k_B T}(1-c)c\right]\frac{\partial c}{\partial \mathbf{r}}\right\} - \frac{\partial}{\partial \mathbf{r}}\left[\frac{D\chi}{k_B T}(1-c)c\frac{\partial^3 c}{\partial \mathbf{r}^3}\right] \quad (14)$$

Neglecting the small correction with the second derivative of c in the desorption term and introducing notations

$$D_{eff}(c) = D\left[1 - \frac{u_0}{k_B T} c(1-c)\right] \quad (15)$$

$$G(c) = \frac{D\chi}{k_B T} c(1-c) \quad (16)$$

we can write this equation in the compact form

$$\frac{\partial c}{\partial t} = k_a p(1-c) - k_{d,0}\, e^{-u_0 c/k_B T} c + \frac{\partial}{\partial \mathbf{r}}\left(D_{eff}(c)\frac{\partial c}{\partial \mathbf{r}}\right) - \frac{\partial}{\partial \mathbf{r}}\left(G(c)\frac{\partial^3 c}{\partial \mathbf{r}^3}\right) \quad (17)$$

Thus, we see that in contrast to usual reaction-diffusion models, this equation contains also terms with the higher third- and fourth-order spatial derivatives. Under normal conditions, these terms can be neglected because they are small as compared with the diffusion term. However, when the phase transition in the adsorbate takes place, the diffusion coefficient $D_{eff}(c)$ becomes negative in a certain interval of coverages c, and to prevent divergencies, the terms with the higher derivatives must be retained.

4. The Phase Transition

As follows from eq 8, the adsorbate coverage in a uniform steady state satisfies the equation

$$k_a p(1-c) - k_{d,0} \exp\left(-\frac{u_0 c}{k_B T}\right) c = 0 \quad (18)$$

which yields the mean-field adsorption isotherm (cf. ref 29). As the temperature is decreased, this equation shows the first-order phase transition leading from the dilute to the dense adsorbate phases. The phase diagram for this transition is presented in Figure 1. In the region II the adsorbate can be found in two phases; i.e., the system is bistable.

The relaxation kinetics of this phase transition is described by eq 8. But, before we discuss the relaxation properties, the relationship between this equation and the thermodynamics of the considered phase transition should be analyzed.

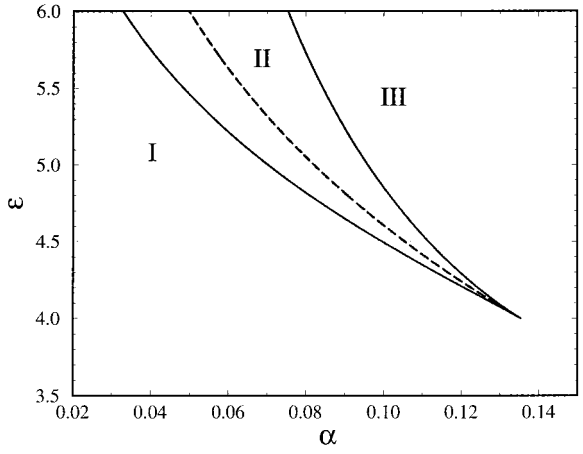

Figure 1. Phase diagram in the plane (ϵ, α) where $\epsilon = u_0/k_B T$ and $\alpha = k_a p/k_{d,0}$. The dilute phase of the adsorbate occupies region I, the dense phase is in region III, and both phases are possible in region II. The dashed line shows the curve of stationary coexistence of the two phases, given by $\alpha = \exp(-\epsilon/2)$.

By introducing the local chemical potential

$$\varphi = -\int u(\mathbf{r}-\mathbf{r}')\, c(\mathbf{r}')\, d\mathbf{r}' + k_B T \ln\left(\frac{c(\mathbf{r})}{1-c(\mathbf{r})}\right) \quad (19)$$

the kinetic equation 8 can be written in the form

$$\frac{\partial c}{\partial t} = k_a p(1-c)\left[1 - \exp\left(\frac{\varphi - \varphi_0}{k_B T}\right)\right] + \frac{\partial}{\partial \mathbf{r}}\left(\frac{D}{k_B T} c(1-c)\frac{\partial \varphi}{\partial \mathbf{r}}\right) \quad (20)$$

where

$$\varphi_0 = k_B T \ln\left(\frac{k_a p}{k_{d,0}}\right) \quad (21)$$

At equilibrium the chemical potential is constant for all parts of the surface and equal to φ_0.

For uniform distributions, the chemical potential is given, according to eq 19, by

$$\varphi(c) = -u_0 c + k_B T \ln\left(\frac{c}{1-c}\right) \quad (22)$$

and, as can readily be seen, the condition $\varphi = \varphi_0$ yields the adsorption isotherm (eq 18). The boundary separating the bistability region II in the phase diagram shown in Figure 1 satisfies the additional condition $d\varphi/dc = 0$ or, explicitly

$$-u_0 + \frac{k_B T}{c(1-c)} = 0 \quad (23)$$

Comparing eq 23 with eq 15 for the effective diffusion coefficient $D_{eff}(c)$, we see that on this boundary $D_{eff}(c)$ changes its sign and becomes negative inside the bistability region. To prevent divergencies, the next term with the higher order derivatives should then be retained in eq 17.

Generally, the interface separating two phases in the region II moves over the surface in such a way that the area covered by the metastable phase decreases. The interface is standing only when an additional Maxwell condition is satisfied. This condition can be derived if we set $\varphi = \varphi_0$ and use approximation 10, thus obtaining for a flat stationary interface the equation

$$-u_0 c + k_B T \ln\left(\frac{c}{1-c}\right) - \chi \frac{\partial^2 c}{\partial x^2} = \varphi_0 \quad (24)$$

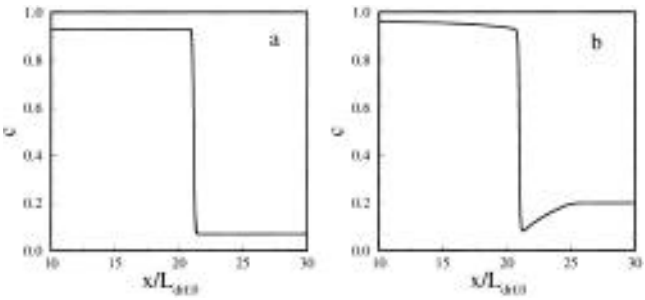

Figure 2. Profiles of the equilibrium standing interface (a) and of a moving interface (b) for $\epsilon = 6$ and $r_0 = 0.1L_{dif,0}$. The standing interface is obtained by numerical integration of eq 24 for $\alpha = \exp(-\epsilon/2) = 0.0498$. The interface, moving to the right, is found by numerical integration of the evolution equation 8 for $\alpha = 0.07753$, for a system of the total length $40L_{dif,0}$.

If we multiply both parts of this equation by the derivative dc/dx and then integrate the result over the coordinate x from $-\infty$ to $+\infty$, we arrive at the usual Maxwell condition for the stationary coexistence of the two phases (ref 29), i.e.

$$\int_{c_1}^{c_2}(\varphi(c) - \varphi_0)\mathrm{d}c = 0 \qquad (25)$$

where the function $\varphi(c)$ is given by eq 22, and c_1 and c_2 are the coverage values in the two phases. In Appendix B we derive the explicit condition (eq B12) that determines the stationary coexistence of two phases.

The profile of the standing interface can be found by integration of eq 24 with boundary conditions $c(x) \rightarrow c_1$ for $x \rightarrow -\infty$ and $c(x) \rightarrow c_2$ for $x \rightarrow +\infty$ when the Maxwell condition (eq 25) is satisfied (Figure 2a). Note that eq 24 does not include the diffusion coefficient D, and because $\chi \approx u_0 r_0^2$, the width of the interface is proportional to the interaction radius r_0. It means that the standing interface separating two phases is very narrow; i.e., its width is about the interaction radius which is much shorter than the diffusion length.[30a]

The stationary coexistence curve of the two phases is shown by the dashed line in Figure 1. On both sides of this curve, the interface is not stationary and moves over the surface. Its motion, together with other effects, such as the growth of a supercritical nucleus, is described by the kinetic equation 8 or its equivalent form (eq 20).

Analyzing the kinetic equation 20, we can notice that its structure is different both from the Ginzburg−Landau equation, describing the relaxation kinetics for first-order phase transitions with nonconserved order parameters, and from the Cahn−Hilliard equation for the phase transition with a conserved order parameter.[31] Though the total adsorbate coverage is conserved in the diffusion process and in the adsorbate flows induced by potential gradients in the surface, the processes of adsorption and desorption do not conserve this quantity.

Figure 2b shows the profile of a steadily moving interface obtained by numerical integration of eq 8. We see that, in contrast to a standing interface, it has a precursor and a tail that extend over a distance much larger than the interaction radius. They appear due to diffusion of the adsorbate, which accompanies motion of an interface, and their lengths are controlled, in the order of magnitude, by the diffusion length.

As the characteristic diffusion length of the problem, the parameter combination $L_{dif,0} = (D/k_{d,0})^{1/2}$ can be used. However, it gives the actual diffusion length only in the limit of very small coverages. The coverages in the two equilibrium phases are greater. According to eq 2, this decreases the desorption rate and therefore makes the effective diffusion length in a particular phase larger. The width of the diffusion-controlled precursor in Figure 2b is, for example, several times greater than $L_{dif,0}$.

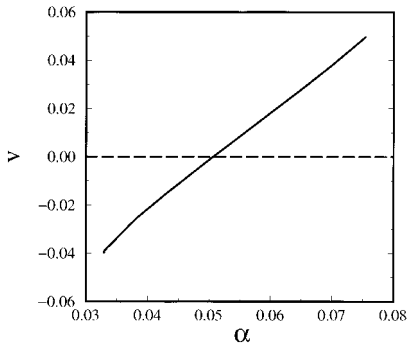

Figure 3. Interface velocity v as function of the parameter α for $\epsilon = 6$ and $r_0 = 0.2L_{dif,0}$. The interface is standing at $\alpha = 0.0498$.

A comment on the algorithm used for the numerical integration of eq 8 is needed. Since this equation is integrodifferential, it is not enough to specify only the values of the coverage, or of its derivative, at the boundary of the medium. When reflecting boundary conditions were used in our simulations, a ribbon of fictitious grid points, of width larger than the interaction radius, has been placed around the actual boundary of the medium. The values of the coverage c in these points have been taken to be equal to the values of c in the respective mirror-reflected grid points inside the medium. The binary attraction potential used in the numerical simulations has been chosen in the form

$$u(r) = \frac{u_0}{\pi r_0^{\,2}} \exp\left(-\frac{r^2}{r_0^{\,2}}\right) \qquad (26)$$

Because of the attractive interaction between the adsorbed molecules, the dense region with high adsorbate coverage acts as a sink sucking the adsorbate from the adjusting low-density region. As a result, the adsorbate distribution in the low-density region in front of the moving phase boundary becomes depleted and the precursor, seen in Figure 2b, is formed. The tail with a decreased adsorbate density, following the interface, is produced due to the "evaporation" of particles out of the dense into the low-density phases. Figure 3 shows the velocity v of the moving interface as a function of the dimensionless parameter $\alpha = k_a p/k_{d,0}$; the velocity is measured in the units of $k_{d,0}L_{dif,0}$.

The consequence of this structure of a moving interface is that when two such interfaces collide, they start to interact at distances much larger than the interaction radius giving the width of the phase boundary, i.e. at distances of about the diffusion length. As seen in Figure 4, their motion is gradually slowed down as the interfaces approach one another.

Hence, though the problem includes only single adsorbate species, two characteristic lengths, i.e. the interaction radius and the diffusion length, become involved when the kinetic processes in the system are considered. In contrast to this, at thermodynamic equilibrium only one characteristic length (the interaction radius) is relevant.

If a strong enough initial perturbation is applied in the spatial region filled by the metastable phase, a nucleus of the stable phase is created. When such nucleus is large, it will grow until the entire surface is transformed into the new stable phase.

The critical nucleus represents a saddle stationary pattern: its slight deformations may produce both growing and shrinking domains. This unstable stationary solution satisfies equation

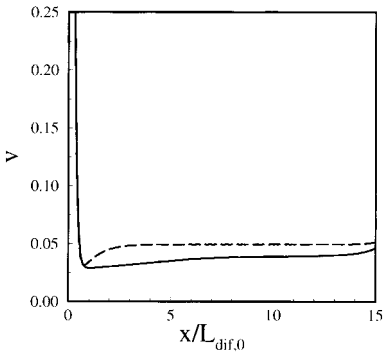

Figure 4. Dependence of the velocity v of two colliding interfaces on the distance $2x$ between them. The dashed curve shows this dependence for the case when $\alpha = 0.07395$, which corresponds to the case where the dilute phase is metastable. The solid curve shows the respective dependence for $\alpha = 0.033$, when the dense phase phase is metastable. Other parameters are the same as in Figure 3.

$$-u_0 c + k_B T \ln\left(\frac{c}{1-c}\right) - \chi \frac{\partial^2 c}{\partial \mathbf{r}^2} = \varphi_0 \qquad (27)$$

with the boundary condition $c(r) \rightarrow c_1$ for $r \rightarrow \infty$ if c_1 is the coverage in the metastable phase.

Therefore, the size of a critical nucleus is controlled by the interaction radius and is not influenced by diffusion. The profiles of a critical nucleus for various values of the parameter $\alpha = k_a p/k_{d,0}$ in the one-dimensional system that have been found by integration of eq 27 are shown in Figure 5.

However, when a nucleus starts to grow, it begins to suck the adsorbate from the adjusting low-density region, and this produces a ring with the depleted adsorbate coverage that surrounds a growing nucleus and is clearly seen in Figure 6. The influence of the growing nucleus extends over a distance about the diffusion length from its border.

Until now our analysis has been based on the macroscopic limit (eq 8) of the mesoscopic evolution equation (eq 7). However, when small-scale spatial patterns, such as growing nuclei, are studied, fluctuations in the system cannot be neglected, and therefore the full mesoscopic equation including the internal noises should be considered.

5. Fluctuations and Stochastic Nucleation

Returning to the mesoscopic evolution equation (eq 5), we see that besides the deterministic terms it includes noises. Their presence reflects the fact that the actual microscopic dynamics of the system is discrete and stochastic, and it is only approximately described using continuous coverage variables. The noises in eq 5 are therefore of "internal" origin: they are neither caused by variations of the system parameters nor by application of external random forces. Retaining such internal noises allows incorporation of microscopic fluctuations into the macroscopic description that is formulated in terms of continuous coverages. Thus, eq 5 can loosely be viewed as a Langevin equation describing the "Brownian motion" of a macroscopic variable (i.e. of the coverage c) under the influence of microscopic stochastic interactions.

Remarkably, the noise terms in eq 5 involve an additional parameter μ that specifies the lattice density, i.e. gives the number of lattice sites per unit surface area. Such a parameter is absent in the macroscopic equations for the coverages, representing fractions of occupied lattice sites. The macroscopic description is not sensitive to the actual number of adsorbate atoms per unit area, corresponding to a given coverage. However, this property becomes very important when fluctuations are considered. Indeed, it is not the coverage but the total number of the involved particles inside a given area that determines the intensity of fluctuations in the number of the atomistic reaction, adsorption, desorption, or diffusion events per unit time in this area.

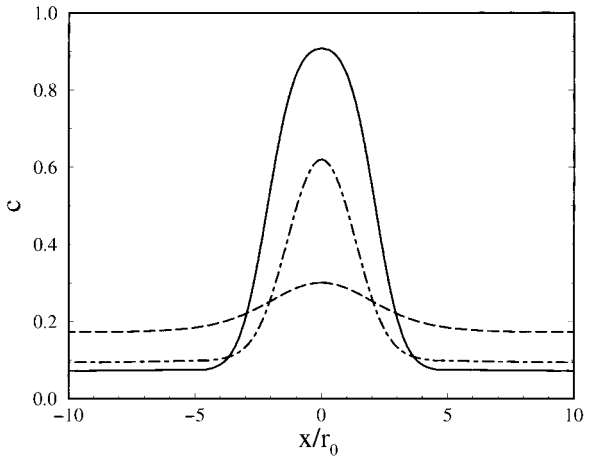

Figure 5. Profiles of critical nuclei for $\epsilon = 6$ and three different values of $\alpha = 0.0499$ (the solid curve, close to the coexistence line), 0.0601 (the dash-dotted curve), and 0.0741 (the dashed curve, close to the absolute stability boundary of the dilute phase) obtained by numerical integration of eq 27 with $\chi/k_B T = \epsilon r_0^2/4$, corresponding to the interaction potential (eq 26).

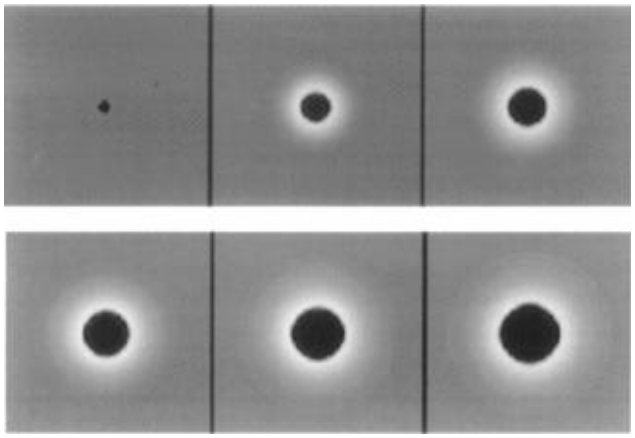

Figure 6. Growth of a nucleus of the dense phase (from top left to bottom right), obtained by numerical integration of eq 8 for $\epsilon = 6$, $\alpha = 0.0753$, and $r_0 = 0.2L_{dif,0}$. The initial radius was chosen to be $1.5r_0$. The system size is $L = 16L_{dif,0}$. The time difference between subsequent snapshots is $\Delta T = 20/k_{d,0}$. The local coverage is plotted in gray scale, decreasing from dark to bright regions.

The mesoscopic evolution equation 5 contains internal noises that correspond to adsorption, desorption, and diffusion, i.e., respectively

$$\phi_a(\mathbf{r},t) = \frac{1}{\mu^{1/2}}[k_a p(1-c)]^{1/2} f_a(\mathbf{r},t) \qquad (28)$$

$$\phi_d(\mathbf{r},t) = \frac{1}{\mu^{1/2}}(k_{d,0} c)^{1/2} \exp\left(\frac{U(\mathbf{r})}{2k_B T}\right) f_d(\mathbf{r},t) \qquad (29)$$

and

$$\phi_{dif}(\mathbf{r},t) = \text{div}\, \mathbf{j}(\mathbf{r},t) \qquad (30)$$

where the random flux $\mathbf{j}(\mathbf{r},t)$ is given by

$$\mathbf{j}(\mathbf{r},t) = \frac{1}{\mu^{1/2}}[2Dc(1-c)]^{1/2} \mathbf{f}(\mathbf{r},t) \qquad (31)$$

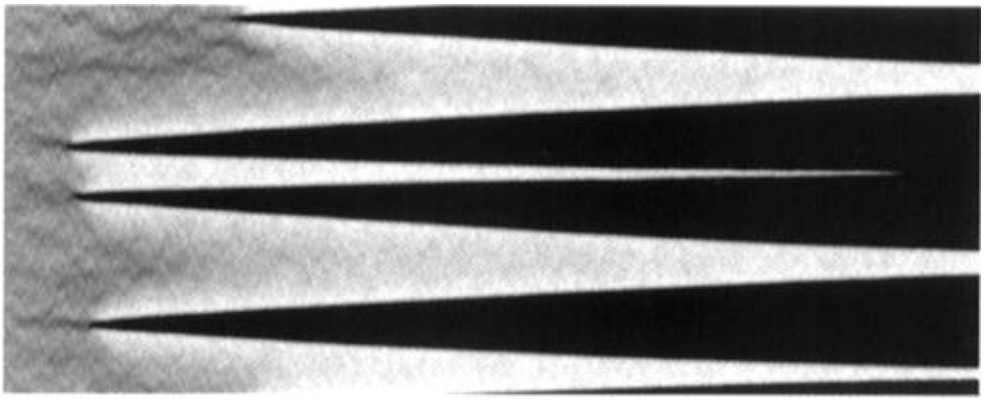

Figure 7. Spontaneous nucleation of the dense phase (black regions) on a dilute background (bright regions) in the one-dimensional system: $\mu = 10^4 L_{\mathrm{dif},0}^{-1}$, $\epsilon = 6$, $\alpha = 0.0753$, and $r_0 = 0.1L_{\mathrm{dif},0}$. The grid size is $\Delta x = 0.02L_{\mathrm{dif},0}$ and the system size is $L = 20L_{\mathrm{dif},0}$. The evolution of the system is shown for a time interval $T = 77/k_{\mathrm{d},0}$ (from left to right).

and the random forces $f_a(\mathbf{r},t)$, $f_d(\mathbf{r},t)$, and $\mathbf{f}(\mathbf{r},t)$ satisfy eqs 7.

Note that the diffusion noise $\phi_{\mathrm{dif}}(\mathbf{r},t)$ is not sensitive to potential interactions between the adsorbed particles. However, its intensity depends on the coverage and is proportional to the product $c(1 - c)$. Hence, this noise becomes weak both for small and large (close to full occupation) coverages. In contrast to the internal noises of adsorption and desorption that represent local fluctuating sources or sinks, the internal noise of diffusion is determined by a local fluctuating flux $\mathbf{j}(\mathbf{r},t)$. The viscous adsorbate flow, induced by the potential gradients over the surface, does not contribute to the noises.

We can estimate the relative intensity of different internal noises. Since all independent random forces f_a, f_d, and $\mathbf{f}$ in eqs 28−31 have the same intensity, it suffices to compare only their prefactors.

At equilibrium, when eq 18 holds, the intensities of the adsorption and desorption noises ϕ_a and ϕ_d are equal. Generally, they have the same order of magnitude, unless very small or very high coverages are considered.

The diffusion noise $\phi_{\mathrm{dif}}(\mathbf{r},t)$ is given, according to eq 30, by the spatial derivative of the random flux $\mathbf{j}(\mathbf{r},t)$. If we decompose this noise into a superposition of fluctuating modes with different wavelengths, the intensity of a mode would depend on its wavelength. In an order of magnitude, we can estimate that, for a characteristic length scale l,

$$\varphi_{\mathrm{dif}} \propto \frac{1}{l\mu^{1/2}}[2Dc(1-c)]^{1/2} \tag{32}$$

On the other hand, the intensity of, e.g., the desorption noise does not depend on the wavelength, and we have

$$\varphi_{\mathrm{d}} \propto \frac{1}{\mu^{1/2}}(k_{\mathrm{d}}c)^{1/2} \tag{33}$$

where $k_d = k_{d,0}\exp(U/k_BT)$ is the desorption rate. By comparing eqs 32 and 33, we see that the diffusion noise dominates over the noise of desorption (and adsorption) on length scales $l < L_{\mathrm{dif}}$ where $L_{\mathrm{dif}} = (D/k_d)^{1/2}$ is the characteristic diffusion length.

The intensity of all internal noises is inversely proportional to the lattice density μ, giving the number of the lattice sites per unit surface area. The derivation of the mesoscopic evolution equation 5 is based (see Appendix A) on the application of the coarse graining procedure, with the condition that each elementary spatial box of a length l_0 contains a large number of particles. Hence, we have the condition $\mu l_0^2 \gg 1$.

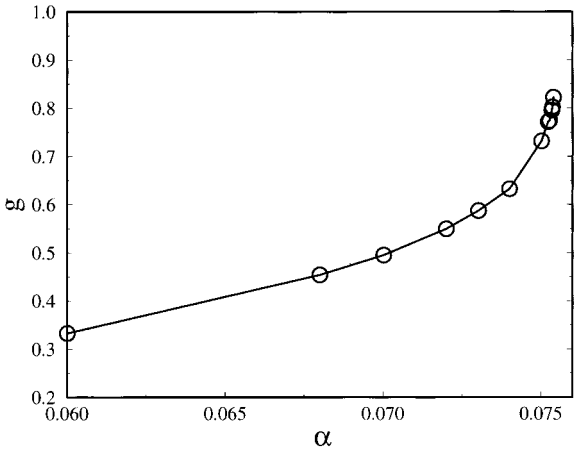

Figure 8. Mean rate g of spontaneous nucleation of a dense nucleus on a dilute background in the one-dimensional model (eq 5) as function of α for $\mu = 10^4 L_{\mathrm{dif},0}^{-1}$, $\epsilon = 6$, and $r_0 = 0.2L_{\mathrm{dif},0}$. The system size is $L = 32L_{\mathrm{dif},0}$, with a grid size $\Delta x = 0.1L_{\mathrm{dif},0}$. This rate is obtained as the mean inverse waiting time (averaged over 10^4 runs) for a supercritical nucleation from a coverage distribution initially homogeneous in the metastable dilute state.

Moreover, the mesoscopic equation can only be applied for the description of processes with the characteristic lengths l that exceed the coarse graining length l_0. The smallest characteristic length of the considered problem is given by the interaction radius r_0. Thus, we see that the mesoscopic approximation is applicable in this problem if the condition $\mu r_0^2 \gg 1$ is satisfied, i.e. if the number of the lattice sites inside the circle of the interaction radius is large.

As has already been noted in section 2, the actual interaction radius usually does not exceed a few lattice lengths, and therefore the product μr_0^2 is actually not very large. When this happens, the mesoscopic theory cannot yield quantitative predictions about the behavior of the system, though it may still be valuable for the qualitative understanding of related phenomena and for the interpretation of experimental data.

An immediate result of the introduction of internal noises is that even in a uniform steady state, local fluctuations of the adsorbate coverage would appear. However, if the system has two uniform steady states (i.e. inside the bistability region in the phase diagram shown in Figure 1), the noises may have even more drastic consequences. By a sufficiently strong local fluctuation, a supercritical nucleus of the new stable phase can be created inside the metastable phase, and thus a phase transition in the system can be triggered. The mesoscopic evolution equation 5 can be used to investigate the process of stochastic nucleation in the system.

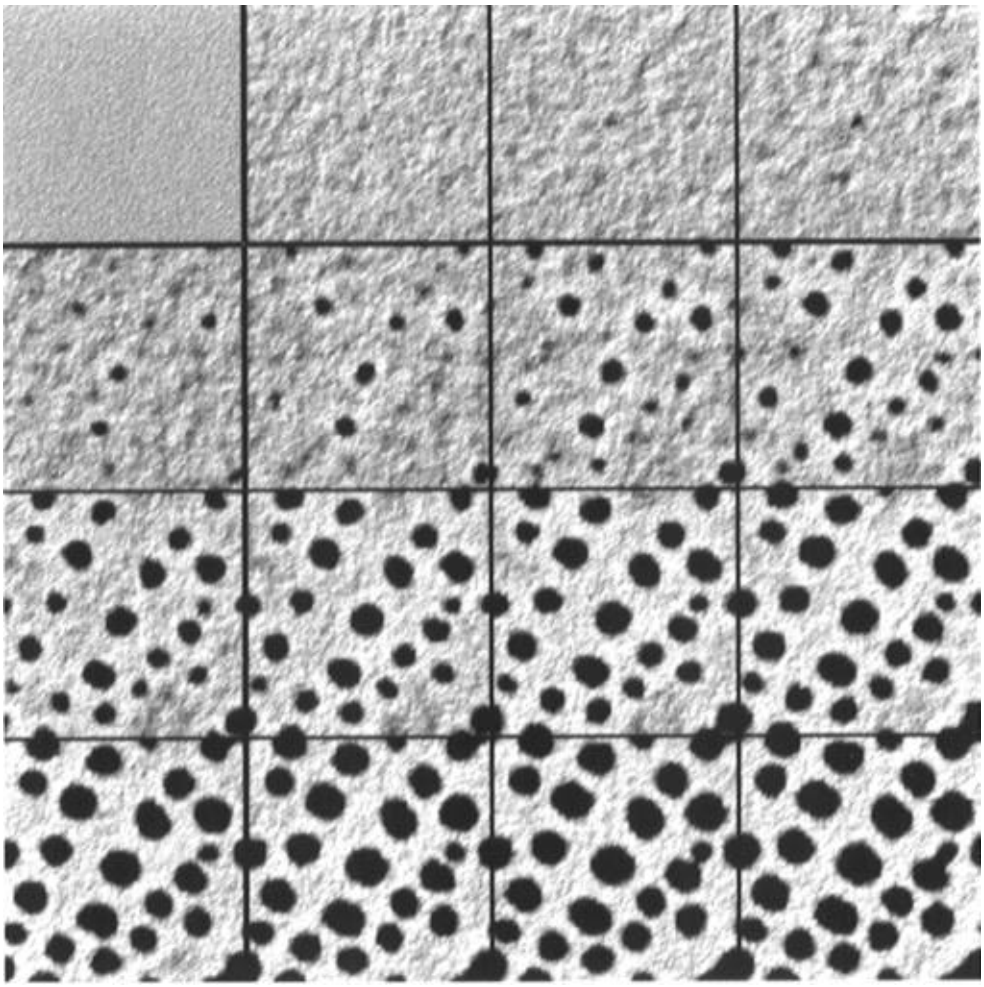

Figure 9. Spontaneous nucleation in the stochastic two-dimensional model (from top left to bottom right). The time interval between subsequent frames is $\Delta T = 5/k_{d,0}$, $\mu = (2 \times 10^3)L_{dif,0}^{-2}$, $\Delta x = 0.1L_{dif,0}$, and all other parameters and notations are the same as in Figure 6.

We have performed numerical integration of the stochastic partial differential equation 5 for one- and two-dimensional systems. After introduction of a grid and replacement of the derivatives by finite differences, the random fields $f_a(\mathbf{r},t)$, $f_d(\mathbf{r},t)$, and $\mathbf{f}(\mathbf{r},t)$ in this equation are modeled by independent Gaussian random variables assigned to each node of the grid at each moment. Their intensities are chosen in such a way that, in the continuous limit, the correlation functions 7 are reproduced.

A detailed statistical analysis of the nucleation phenomena in adsorbates with attractive lateral interactions will be subject of a forthcoming publication. Below we only illustrate the application of mesoscopic stochastic modeling in studies of such processes.

In a typical simulation, a uniform state corresponding to the metastable dilute phase of the adsorbate is chosen as the initial condition. As seen in Figure 7 for the one-dimensional case, fluctuations of various sizes appear on the background of this stationary state, as a result of the noise action. Eventually, a strong fluctuation is created that gives rise to a supercritical nucleus. Once such a nucleus is formed, it continues to grow in a deterministic manner, and the region filled by the new stable phase spreads over the entire medium (Figure 7).

To estimate the stochastic nucleation rate, the following procedure has been adopted: We have always started from the same uniform steady state and integrated the evolution equation until a supercritical nucleus of a given fixed size has developed. When this has occurred, further integration has been stopped and the time T_0 passed from the beginning of the process until this event has been recorded. By repeating the simulations, we have found the statistical distribution of the nucleation times T_0 for the chosen parameter values. The statistical average of $1/T_0$ gives then the mean nucleation rate. Figure 8 shows the computed dependence of the nucleation rate on the parameter $\alpha = k_a p/k_{d,0}$ in the one-dimensional system. As can be expected, the nucleation rate diverges when the bistability boundary in the phase diagram (Figure 1) is approached.

The numerical simulations of stochastic nucleation in two-dimensional systems require larger computation time, and, in this paper, we present only an example of a simulation showing the early stage of this process (Figure 9). In the beginning, individual islands of the dense phase appear in the system. As such islands grow and their number increases, they start to interact. The interaction is caused by the depletion of the adsorbate in the region surrounding a growing island, which has earlier been seen in Figure 6. As a consequence, the islands tend to keep a certain spacing, and formation of new small nuclei in the regions between the islands is prevented. Note that fluctuations in this region are also suppressed.

This effect resembles the phenomenon of the Ostwald ripening in the vapor−liquid first-order phase transitions which is described at its late stage by the Lifshitz−Slyozov theory.[32] However, the total mass of the adsorbate is not conserved in the system considered. Indeed, the processes of adsorption and desorption tend to bring the local adsorbate coverage to the equilibrium level. As a consequence, as has been noted in section 4, the influence of a moving interface cannot extend

further than the diffusion length L_{dif}. It means that two islands can interact only if they are separated by a distance which is less than this characteristic length. If we look at Figure 9, it can be noticed that, in an order of magnitude, the mean distance between the islands is close to L_{dif}.

The subsequent growth of the islands should lead to their final fusion and formation of a uniform state with small statistical fluctuations. This last stage is very slow because the speed of the interface boundaries is then greatly decreased.

6. Conclusions

Using the example of an adsorbate with attractive lateral interactions between molecules, we have shown in this paper how a mesoscopic evolution equation for the local fluctuating coverage can be constructed. The analysis of this equation has revealed that it remains valid after the phase transition, when two adsorbate phases exist and the diffusion equation is no longer applicable because the diffusion constant is negative. The mesoscopic equation yields, as its special solution, the thermodynamic equilibrium for the considered system. Moreover, it describes the processes of relaxation to the equilibrium state and, particularly, the motion of interfaces. The internal noises present in the mesoscopic equation give rise to statistical fluctuations in the local adsorbate coverage. They also account for the spontaneous generation of nuclei of the new stable phase and thus allow investigation of the phenomena of stochastic nucleation in this phase transition and direct determination of the kinetic nucleation rate.

The proposed approach is based on the local mean-field approximation and does not allow consideration of discrete lattice effects (though the parameter giving the density of lattice sites already enters into the stochastic mesoscopic equation). Because of this, it is best suited for the description of spatiotemporal pattern formation at mesoscales, i.e. for the processes whose characteristic length scales are larger than the lattice length but might be less than the diffusion length of the problem.

As we have seen, even a single structure, such as a moving interface or a growing island, may include two different length scales: the short radius of attractive interactions and the long diffusion length. The presence of such two length scales is essential for understanding the collective dynamics of large populations of such structures.

Although we have considered in this paper only a simple example of an adsorbate formed by a single kind of molecule without any chemical reactions, the employed method can be generalized to describe more complex situations. Examples of the application of mesoscopic models in studies of chemical reactions in the adsorbates will be given in our forthcoming publications.

Acknowledgment. The authors are grateful to G. Ertl for stimulating discussions. We also acknowledge valuable discussions with R. S. Berry, R. Kapral, Ya. Kevrekides, and L. Schmidt.

Appendix A

In this Appendix we derive from the microscopic master equation 4 the mesoscopic stochastic evolution equation 5. To simplify the notations, the derivation is carried out for a one-dimensional system, but it can straightforwardly be generalized to the two-dimensional case.

We introduce the coarse-grained description and divide the entire lattice into m boxes, each containing a large number N_{max} of sites, which are still small as compared to the minimal characteristic length scale of the appearing spatial patterns. Complete diffusional mixing is assumed to take place inside every such box.

The total probabilities per unit time for the occurrence of an adsorption or desorption event in a box j already containing n_j particles are proportional to the number of empty or, respectively, occupied lattice sites in this box and are therefore given by the equations

$$\tilde{w}^{a}(n_j) = w^{a}\,(N_{max} - n_j) \tag{A1}$$

$$\tilde{w}^{d}(n_j) = w_j^{d} n_j \tag{A2}$$

where the probabilities of adsorption and desorption for a single (empty or, respectively, occupied) lattice site are

$$w^{a} = k_a p \tag{A3}$$

$$w_j^{d} = k_{d,0} \exp(U_j/k_B T) \tag{A4}$$

Other notations have been introduced in section 2. We assume that the potential $U(\mathbf{r})$ does not significantly change inside a box j, and therefore it can be characterized there by a certain value U_j.

The mobility of adsorbed particles is described as a random walk of particles on a chain of boxes. In the presence of potential interactions, the hopping rates of the particles are asymmetric. The probability fluxes for the jth box can be schematically represented as

$$[j-1] \underset{\tilde{w}_j^-}{\overset{\tilde{w}_{j-1}^+}{\rightleftarrows}} [j] \underset{\tilde{w}_{j+1}^-}{\overset{\tilde{w}_j^+}{\rightleftarrows}} [j+1] \tag{A5}$$

Under the assumption of complete mixing inside the boxes, the probabilities per unit time $\tilde{w}_j^{\pm}$ for a transition between the neighboring boxes are proportional to the number n_j of particles in the jth box and to the fraction $(1 - n_{j\pm1})/N_{max}$ of empty sites in the target box. Thus we have

$$\tilde{w}_j^{\pm} = w_j^{\pm}\left(1 - \frac{n_{j\pm1}}{N_{max}}\right) n_j \tag{A6}$$

where the hopping rates for a single particle into a free site in the adjacent box are given (cf. eq 2) by

$$w_j^{\pm} = \begin{cases} \nu \exp\left(\dfrac{U_j - U_{j\pm1}}{k_B T}\right), & \text{if } U_j < U_{j\pm1} \\ \nu, & \text{if } U_j > U_{j\pm1} \end{cases} \tag{A7}$$

and ν is the hopping rate between the boxes.

Thus, we obtain the master equation for the multidimensional distribution $p(\{n_1,...,n_m\},t)$, which gives the probability of finding

$n_1,...,n_m$ particles in the boxes located at $x_1,...,x_m$ at moment t:

$$\frac{\partial p}{\partial t}(\{n_j\},t) = w^a\sum_j[(N_{max}-n_j+1)\tilde{p}_j^- - (N_{max}-n_j)p(\{n_j\},t)] + \sum_j w_j^d[(n_j+1)\tilde{p}_j^+ - n_j p(\{n_j\},t)] + \sum_j[w_{j-1}^+(n_{j-1}+1)p_{j-1}^+ + w_{j+1}^-(n_{j+1}+1)p_{j+1}^-]\left(1-\frac{n_j-1}{N_{max}}\right) - \sum_j\left[w_j^+\left(1-\frac{n_{j+1}}{N_{max}}\right)+w_j^-\left(1-\frac{n_{j-1}}{N_{max}}\right)\right]n_j p(\{n_j\},t) \quad (A8)$$

Here and below the sums over j are taken from 1 to m and the following shorthand notations are employed:

$$\tilde{p}_j^- = p(\{n_1,...,n_j-1,...,n_m\},t)$$

$$\tilde{p}_j^+ = p(\{n_1,...,n_j+1,...,n_m\},t)$$

$$p_j^- = p(\{n_1,...,n_{j-1}-1,n_j+1,...,n_m\},t)$$

$$p_j^+ = p(\{n_1,...,n_j+1,n_{j+1}-1,...,n_m\},t) \quad (A9)$$

After shifting the summation index j in the third sum in eq A8 and introduction of the notations

$$\sigma_j = \frac{w_j^+ + w_j^-}{2} \quad (A10)$$

and

$$\gamma_j = \frac{w_j^+ - w_j^-}{2} \quad (A11)$$

the master equation (A8) takes the form

$$\frac{\partial p}{\partial t}(\{n_j\},t) = w^a\sum_j[(N_{max}-n_j+1)\tilde{p}_j^- - (N_{max}-n_j)p(\{n_j\},t)] + \sum_j w_j^d[(n_j+1)\tilde{p}_j^+ - n_j p(\{n_j\},t)] + \sum_j\left[\sigma_j(n_j+1)\left\{\left(1-\frac{n_{j+1}-1}{N_{max}}\right)p_j^+ + \left(1-\frac{n_{j-1}-1}{N_{max}}\right)p_j^-\right\}\right] - \sum_j\left[\sigma_j n_j\left(2-\frac{n_{j+1}+n_{j-1}}{N_{max}}\right)p(\{n_j\},t)\right] + \sum_j\left[\gamma_j(n_j+1)\left\{\left(1-\frac{n_{j+1}-1}{N_{max}}\right)p_j^+ - \left(1-\frac{n_{j-1}-1}{N_{max}}\right)p_j^-\right\}\right] + \sum_j\left[\gamma_j n_j\left(\frac{n_{j+1}-n_{j-1}}{N_{max}}\right)p(\{n_j\},t)\right] \quad (A12)$$

Now we use our assumption that the number of lattice sites N_{max} in each box is large (i.e. $N_{max} \gg 1$). Introducing the local coverages $c_j = n_j/N_{max}$ and taking into account that the coverage changes only a little as a result of an adsorption, desorption of hopping event that involves a single particle, we write approximately that

$$\tilde{p}_j^\pm \approx P \pm \frac{1}{N_{max}}\frac{\partial P}{\partial c_j} + \frac{1}{2N_{max}^2}\frac{\partial^2 P}{\partial c_j^2} \quad (A13)$$

$$p_j^\pm \approx P + \frac{1}{N_{max}}\left\{\frac{\partial P}{\partial c_j} - \frac{\partial P}{\partial c_{j\pm1}}\right\} + \frac{1}{N_{max}^2}\left\{\frac{1}{2}\frac{\partial^2 P}{\partial c_j^2} + \frac{1}{2}\frac{\partial^2 P}{\partial c_{j\pm1}^2} - \frac{\partial^2 P}{\partial c_j \partial c_{j\pm1}}\right\} \quad (A14)$$

where P is a short notation for the distribution function $P(\{c_j\})$. Substituting these approximations into eq A12 and retaining there the terms up to the order $1/N_{max}$, we obtain a multidimensional Fokker−Planck equation for the joint probability distribution $P(\{c_j\})$. This equation has the form

$$\frac{\partial P}{\partial t}(\{c_j\},t) = -\sum_j\frac{\partial}{\partial c_j}[w^a(1-c_j)P] + \frac{1}{2N_{max}}\sum_j\frac{\partial^2}{\partial c_j^2}[w^a(1-c_j)P] - \sum_j\frac{\partial}{\partial c_j}[-w_j^d c_j P] + \frac{1}{2N_{max}}\sum_j\frac{\partial^2}{\partial c_j^2}[w_j^d c_j P] - \sum_j\frac{\partial}{\partial c_j}[(\sigma_{j+1}c_{j+1}+\sigma_{j-1}c_{j-1}-2\sigma_j c_j)(1-c_j)P] - \sum_j\frac{\partial}{\partial c_j}[(c_{j+1}+c_{j-1}-2c_j)\sigma_j c_j P] + \frac{1}{2N_{max}}\sum_j\frac{\partial^2}{\partial c_j^2}[\{(\sigma_{j+1}c_{j+1}+\sigma_{j-1}c_{j-1}-2\sigma_j c_j)(1-c_j) - (c_{j+1}+c_{j-1}-2c_j)\sigma_j c_j\}P] - \frac{1}{N_{max}}\sum_j\frac{\partial}{\partial c_j}\left\{\frac{\partial}{\partial c_{j+1}}(1-c_{j+1}) + \frac{\partial}{\partial c_{j-1}}(1-c_{j-1}) - 2\frac{\partial}{\partial c_j}(1-c_j)\right\}[\sigma_j c_j P] - \sum_j\frac{\partial}{\partial c_j}[\{\gamma_j c_j(c_{j+1}-c_{j-1}) + (c_j-1)(\gamma_{j+1}c_{j+1}-\gamma_{j-1}c_{j-1})\}P] - \frac{1}{2N_{max}}\sum_j\frac{\partial^2}{\partial c_j^2}[\{\gamma_j c_j(c_{j+1}-c_{j-1}) + (1-c_j)(\gamma_{j+1}c_{j+1}-\gamma_{j-1}c_{j-1})\}P] - \frac{1}{N_{max}}\sum_j\frac{\partial}{\partial c_j}\left\{\frac{\partial}{\partial c_{j+1}}(1-c_{j+1}) - \frac{\partial}{\partial c_{j-1}}(1-c_{j-1})\right\}[\gamma_j c_j P] \quad (A15)$$

As mentioned earlier in this Appendix, the size of an individual box (which is denoted below by l_0) is small as compared to the minimal characteristic scale of the considered spatial patterns. Therefore the coverages c_j do not significantly change between the neighboring boxes and can be viewed as the values of a certain smooth coverage $c(x)$, taken at discrete coordinate points.

This notion allows us to introduce a continuous version of eq A15 in terms of a smooth coverage $c(x)$. After the transformation to continuous coordinates, the multidimensional distribution function $P(\{c_i\},t)$ converts into a functional $P([c(x)],t)$

that gives the probability density of various realizations of the random coverage field $c(x)$. The evolution equation for this functional is

$$\frac{\partial P}{\partial t} = -\int \mathrm{d}x \frac{\delta}{\delta c(x)}\left\{\left[w^{\mathrm{a}}(1-c) - w^{\mathrm{d}}c + 2l_0\frac{\partial(\gamma c(1-c))}{\partial x}\right]P([c(x)],t)\right\} - l_0^2\int \mathrm{d}x\frac{\delta}{\delta c(x)}\left\{\left[(1-c)\frac{\partial^2(\sigma c)}{\partial x^2} + \sigma c\frac{\partial^2 c}{\partial x^2}\right]P([c(x)],t)\right\} + \frac{1}{2\mu}\int \mathrm{d}x \frac{\delta^2}{\delta c(x)^2}\left\{\left[w^{\mathrm{a}}(1-c) + w^{\mathrm{d}}c + l_0^2(1-c)\frac{\partial^2(\sigma c)}{\partial x^2} - \sigma l_0^2 c\frac{\partial^2 c}{\partial x^2}\right]P([c(x)],t)\right\} + \frac{l_0}{2\mu}\int \mathrm{d}x \frac{\delta^2}{\delta c(x)^2}\left\{\left[2\gamma c\frac{\partial c}{\partial x} - 2(1-c)\frac{\partial(\gamma c)}{\partial x}\right]P([c(x)],t)\right\} - \frac{l_0^2}{\mu}\int \mathrm{d}x \frac{\delta}{\delta c(x)}\frac{\partial^2}{\partial x^2}\left(\frac{\delta}{\delta c(x)}(1-c)\right)\{\sigma c P([c(x)],t)\} - \frac{l_0}{\mu}\int \mathrm{d}x \frac{\partial}{\partial x}\left(\left[\frac{\delta}{\delta c(x)}\right]^2\right)\{\gamma c(1-c)P([c(x)],t)\} \quad \text{(A16)}$$

Here, we have introduced the parameter $\mu = N_{\max}/l_0$ that gives the number of lattice sites per unit area.

The coefficients σ and γ in eq A16 represent certain functions of the coordinate x that are given by the equations [cf. eqs A8, A10, and A11]

$$\sigma(x) = \frac{\nu}{2}\left[1 + \exp\left(-\frac{l_0}{k_{\mathrm{B}}T}\left|\frac{\partial U}{\partial x}\right|\right)\right] \quad \text{(A17)}$$

$$\gamma(x) = -\frac{\nu}{2}\left[1 - \exp\left(-\frac{l_0}{k_{\mathrm{B}}T}\left|\frac{\partial U}{\partial x}\right|\right)\right]\mathrm{sign}\left(\frac{\partial U}{\partial x}\right) \quad \text{(A18)}$$

In the limit when $l_0 \to 0$ we therefore get

$$\lim_{l_0\to 0}(\sigma(x)l_0^2) = D \quad \text{(A19)}$$

where D is the diffusion constant

$$D = \lim_{l_0\to 0}(\nu l_0^2) \quad \text{(A20)}$$

and

$$\lim_{l_0\to 0}(\gamma(x)l_0) = \lim_{l_0\to 0}\left(-\frac{\nu l_0^2}{2k_{\mathrm{B}}T}\frac{\partial U}{\partial x}\right) = -\frac{1}{2}\frac{D}{k_{\mathrm{B}}T}\frac{\partial U}{\partial x} \quad \text{(A21)}$$

If we introduce the functional differential operator

$$\hat{A}(x) = \frac{\delta}{\delta c(x)} \quad \text{(A22)}$$

and take in eq A16 the limit $l_0 \to 0$, we obtain, using eqs A19 and A21, the equation

$$\frac{\partial P}{\partial t} = -\int \mathrm{d}x\, \hat{A}(x)\left[w^{\mathrm{a}}(1-c) - w^{\mathrm{d}}c + \frac{\partial}{\partial x}\left(\frac{D}{k_{\mathrm{B}}T}\frac{\partial U}{\partial x}c(1-c)\right) + D\frac{\partial^2 c}{\partial x^2}\right]P + \frac{1}{2\mu}\int \mathrm{d}x\, \hat{A}^2(x)\left[w^{\mathrm{a}}(1-c) + w^{\mathrm{d}}c + D(1-2c)\frac{\partial^2 c}{\partial x^2} - \frac{Dc}{k_{\mathrm{B}}T}\frac{\partial U}{\partial x}\frac{\partial c}{\partial x} + (1-c)\frac{\partial}{\partial x}\left(\frac{Dc}{k_{\mathrm{B}}T}\frac{\partial U}{\partial x}\right)\right]P - \frac{D}{\mu}\int \mathrm{d}x\left[\hat{A}(x)\frac{\partial^2}{\partial x^2}(\hat{A}(x)(1-c))c - \frac{1}{2}\frac{\partial}{\partial x}(\hat{A}^2(x))\frac{1}{k_{\mathrm{B}}T}c(1-c)\frac{\partial U}{\partial x}\right]P \quad \text{(A23)}$$

To bring this equation into the form of a functional Fokker–Planck equation for the probability functional P, certain transformations must be performed.

Let us first consider the terms in eq A23 that are inversely proportional to μ and independent of the potential U, i.e.

$$F_{\mathrm{d}} = \frac{D}{\mu}\int \mathrm{d}x\left\{\hat{A}^2(x)\left[\frac{1}{2}(1-2c)\frac{\partial^2 c}{\partial x^2}\right] - \hat{A}(x)\frac{\partial^2}{\partial x^2}[\hat{A}(x)(1-c)]c\right\}P \quad \text{(A24)}$$

This expression can be further transformed as

$$\begin{aligned} F_{\mathrm{d}} &= \frac{D}{\mu}\int \mathrm{d}x\left\{\hat{A}^2(x)\left[\frac{1}{2}(1-2c)\frac{\partial^2 c}{\partial x^2} + c\frac{\partial^2 c}{\partial x^2}\right] + 2\hat{A}(x)\frac{\partial \hat{A}(x)}{\partial x}\frac{\partial c}{\partial x}c - \hat{A}(x)\frac{\partial^2}{\partial x^2}[\hat{A}(x)](1-c)c\right\}P \\ &= \frac{D}{\mu}\int \mathrm{d}x\left\{\hat{A}^2(x)\left[\frac{1}{2}\frac{\partial^2 c}{\partial x^2}\right] + \frac{\partial \hat{A}^2(x)}{\partial x}\frac{\partial c}{\partial x}c - \frac{1}{2}\frac{\partial^2}{\partial x^2}[\hat{A}^2(x)](1-c)c + \left[\frac{\partial \hat{A}}{\partial x}\right]^2(1-c)c\right\}P \\ &= \frac{D}{\mu}\int \mathrm{d}x\left\{\hat{A}^2(x)\left[\frac{1}{2}\frac{\partial^2 c}{\partial x^2}\right] + \frac{1}{2}\frac{\partial \hat{A}^2(x)}{\partial x}\frac{\partial c}{\partial x} + \left[\frac{\partial \hat{A}}{\partial x}\right]^2(1-c)c\right\}P \\ &= \frac{D}{\mu}\int \mathrm{d}x\left(\frac{\partial \hat{A}}{\partial x}\right)^2 c(1-c)P = \frac{D}{\mu}\int\int \mathrm{d}x\mathrm{d}y\frac{\partial \hat{A}(x)}{\partial x}\frac{\partial \hat{A}(y)}{\partial y}c(x)(1-c(x))\delta(x-y)P \\ &= \frac{1}{2\mu}\int\int \mathrm{d}x\mathrm{d}y\,\hat{A}(x)\,\hat{A}(y)\frac{\partial^2}{\partial x\partial y}[2Dc(x)(1-c(x))\delta(x-y)]P \end{aligned} \quad \text{(A25)}$$

Note that we have several times used above integration by parts to arrive at the final expression for F_{d}.

Next, we consider the terms of order $O(\mu^{-1})$ in eq A23 that are proportional to the gradient of the potential U. We find that such terms cancel each other, i.e.

$$F_{\mathrm{u}} = \frac{D}{2\mu k_{\mathrm{B}}T}\int \mathrm{d}x\left\{\hat{A}^2(x)\left[-\frac{\partial U}{\partial x}c\frac{\partial c}{\partial x} + (1-c)\frac{\partial}{\partial x}\left(c\frac{\partial U}{\partial x}\right)\right] + \frac{\partial}{\partial x}(\hat{A}^2(x))c(1-c)\frac{\partial U}{\partial x}\right\}P$$

$$= \frac{D}{2\mu k_B T}\int dx\, \hat{A}^2(x)\Big[-\frac{\partial U}{\partial x}\, c\, \frac{\partial c}{\partial x} + (1-c)\frac{\partial}{\partial x}\Big(c\frac{\partial U}{\partial x}\Big) - \frac{\partial}{\partial x}\Big(c(1-c)\frac{\partial U}{\partial x}\Big)\Big]P = 0 \quad \text{(A26)}$$

Using eqs A25 and A26 and returning to the original full notations, we can therefore write the evolution equation A23 as

$$\frac{\partial P}{\partial t} = -\int dx\, \frac{\delta}{\delta c(x)}\Big\{\Big[w^a(1-c) - w^d(x)c + \frac{D}{k_B T}\frac{\partial}{\partial x}\Big(c(1-c)\frac{\partial U}{\partial x}\Big) + D\frac{\partial^2 c}{\partial x^2}\Big]P\Big\} + \frac{1}{2\mu}\int\int dx\, dy \frac{\delta^2}{\delta c(x)\,\delta c(y)}\Big\{\Big[(w^a(1-c) + w^d(x)c)\delta(x-y) + \frac{\partial^2}{\partial x \partial y}(2Dc(1-c)\delta(x-y))\Big]P\Big\} \quad \text{(A27)}$$

We see that it represents the functional Fokker−Planck equation for the probability distribution $P([c(x)],t)$. As follows from the theory of random processes (cf. refs 24−26), this Fokker-Planck equation is equivalent to the stochastic partial differential equation for the fluctuating field $c(x,t)$ that has the form

$$\frac{\partial c}{\partial t} = w^a(1-c) - w^d(x)c + \frac{D}{k_B T}\frac{\partial}{\partial x}\Big(c(1-c)\frac{\partial U}{\partial x}\Big) + D\frac{\partial^2 c}{\partial x^2} + \frac{1}{\mu^{1/2}}[w^a(1-c)]^{1/2} f_a(x,t) + \frac{1}{\mu^{1/2}}[w^d(x)]^{1/2} f_d(x,t) + \frac{1}{\mu^{1/2}}\frac{\partial}{\partial x}[(2Dc(1-c))^{1/2} f(x,t)] \quad \text{(A28)}$$

where $f_a(x,t)$, $f_d(x,t)$, and $f(x,t)$ are independent white noises of unit intensity and the Ito interpretation of the stochastic differential equation is chosen. Equation A28 represents the one-dimensional version of the mesoscopic evolution equation 5. Thus, by proceeding from the microscopic master equation of the lattice model, we have derived this equation. The generalization of this derivation to the two-dimensional case is straightforward.

Appendix B

In this Appendix we analytically determine the line of stationary coexistence of the dense and dilute phases, given by the Maxwell condition 25.

Performing the integration in eq 25, it can be written as

$$-\frac{u_0 c_1^2}{2} + k_B T \ln(1-c_1) + k_B T c_1 \ln\Big(\frac{c_1}{1-c_1}\Big) - \varphi_0 c_1 = -\frac{u_0 c_2^2}{2} + k_B T \ln(1-c_2) + k_B T c_3 \ln\Big(\frac{c_2}{1-c_2}\Big) - \varphi_0 c_2 \quad \text{(B1)}$$

where c_1 and c_2 are the equilibrium coverages in the two phases that satisfy the equations

$$-u_0 c_1 + k_B T \ln\Big(\frac{c_1}{1-c_1}\Big) = \varphi_0 \quad \text{(B2)}$$

$$-u_0 c_2 + k_B T \ln\Big(\frac{c_2}{1-c_2}\Big) = \varphi_0 \quad \text{(B3)}$$

and φ_0 is given by

$$\varphi_0 = k_B T \ln\Big(\frac{k_a p}{k_{d,0}}\Big) \quad \text{(B4)}$$

The system of equations B1−B3 determines the condition of stationary coexistence of the two phases and the values of the adsorbate coverage in the two coexisting phases.

Multiplying eqs B2 and B3 by c_1 and c_2, respectively, we obtain

$$k_B T c_1 \ln\Big(\frac{c_1}{1-c_1}\Big) - \varphi_0 c_1 = u_0 c_1^2 \quad \text{(B5)}$$

$$k_B T c_2 \ln\Big(\frac{c_2}{1-c_2}\Big) - \varphi_0 c_2 = u_0 c_2^2 \quad \text{(B6)}$$

Substitution of eqs B5 and B6 into eq B1 leads to the equation

$$\frac{u_0(c_2^2 - c_1^2)}{2} + k_B T \ln\Big(\frac{1-c_2}{1-c_1}\Big) = 0 \quad \text{(B7)}$$

Subtracting eq B3 from eq B2, we find the equation

$$u_0(c_2 - c_1) + k_B T \ln\Big(\frac{c_1}{c_2}\Big) = k_B T \ln\Big(\frac{1-c_2}{1-c_1}\Big) \quad \text{(B8)}$$

Subtraction of eq B7 from eq B8 leads to the new equation

$$\frac{1}{2}u_0[(1-c_2)^2 - (1-c_1)^2] + k_B T \ln\Big(\frac{c_2}{c_1}\Big) = 0 \quad \text{(B9)}$$

The system of equations B2, B7, and B9 is equivalent to the system B1−B3. Its examination allows us to notice that its solutions satisfy the condition $c_1 + c_2 = 1$. When this condition is applied, eq B7 reduces to eq B9. Substituting $c_2 = 1 - c_1$ into eq B9 yields

$$-u_0 c_1 + k_B T \ln\Big(\frac{c_1}{1-c_1}\Big) = -\frac{1}{2}u_0 \quad \text{(B10)}$$

Comparing eqs B2 and B10, we see that

$$\varphi_0 = -\frac{1}{2}u_0 \quad \text{(B11)}$$

Taking now into account the definition (eq B4) of φ_0, we thus finally derive an explicit condition determining the coexistence of the two phases

$$k_a p = k_{d,0} \exp\Big(-\frac{u_0}{2k_B T}\Big) \quad \text{(B12)}$$

The coexistence line of two phases, given by eq B12, is plotted as the dashed curve in the phase diagram in Figure 1.

References and Notes

(1) Zambelli, T.; Trost, J.; Wintterlin, J.; Ertl, G. *Phys. Rev. Lett.* **1996**, *76*, 795.
(2) Gorodetskii, V.; Lauterbach, J.; Rotermund, H. A.; Block, J. H.; Ertl, G. *Nature* **1994**, *370*, 276.
(3) Nørskov, J. K. In *Coadsorbtion, Promoters and Poisons*; King, D. A., Woodruff, D. P., Eds.; Elsevier: Amsterdam, 1993; p 1.
(4) Einstein, T. L.; Schrieffer, J. R. *Phys. Rev. B* **1973**, *7*, 3629.
(5) Lau, K. H.; Kohn, W. *Surf. Sci.* **1978**, *75*, 69.
(6) Zeppenfeld, P.; Krzyzowski, M.; Romainczyk, C.; Gomsa, G.; Lagally, M. G. *Phys. Rev. Lett.* **1994**, *72*, 2737.
(7) Marchenko, V. I. *JETP Lett.* **1991**, *67*, 855.
(8) Vanderbilt, D. *Surf. Sci.* **1992**, *268*, L300.
(9) Mikhailov, A.; Ertl, G. *Science* **1996**, *272*, 1596.

(10) de Gennes, P. G. *Rev. Mod. Phys.* **1985**, *57*, 827.
(11) Heckl, W. M.; Möhwald, H. *Ber. Bunsen-Ges. Phys. Chem.* **1986**, *90*, 1159.
(12) Mikhailov, A. *Foundations of Synergetics. I. Distributed Active Systems*; Springer: Berlin, Heidelberg, 1990; 2nd revised ed., 1994.
(13) Krischer, K.; Eiswirth, M.; Ertl, G. *Surf. Sci.* **1991**, *251/252*, 900.
(14) Eiswirth, M.; Ertl, G. In *Chemical Waves and Patterns*; Kapral, R., Showalter, K., Eds.; Kluwer: Dordrecht, 1995; p 447.
(15) Rose, K. C.; Battogtokh, D.; Mikhailov, A.; Imbihl, R.; Engel, W.; Bradshaw, A. M. *Phys. Rev. Lett.* **1996**, *76*, 3582.
(16) Khrustova, N.; Veser, G.; Mikhailov, A.; Imbihl, R. *Phys. Rev. Lett.* **1995**, *75*, 3564.
(17) Ziff, R.; Gulari, E.; Barshad, Y. *Phys. Rev. Lett.* **1986**, *56*, 2553.
(18) Wu, X.-G.; Kapral, R. *Physica A* **1992**, *188*, 284.
(19) Sadig, A.; Binder, K. *Surf. Sci.* **1983**, *128*, 350.
(20) Fichthorn, K.; Gulari, E.; Ziff, R. *Phys. Rev. Lett.* **1989**, *63*, 1527.
(21) Rose, H.; Hempel, H.; Schimansky-Geier, L. *Physica A* **1994**, *206*, 421.
(22) Evans, J. W. *J. Chem. Phys.* **1992**, *97*, 572. See also the following. Tammaro, M.; Sabella, M.; Evans, J. W. *J. Chem. Phys.* **1995**, *103*, 10277.
(23) Kreuzer, H. J. *Phys. Rev. B* **1991**, *44*, 1232.
(24) Gardiner, G. W. *Handbook of Stochastic Methods*; Springer: Berlin, Heidelberg, 1985).
(25) Mikhailov, A. *Phys. Rep.* **1989**, *184*, 308.
(26) Mikhailov, A.; Loskutov, A. *Foundations of Synergetics. II. Chaos and Noise* Springer: Berlin, Heidelberg, 1991; 2nd revised ed., 1996.
(27) Wu, X.-G.; Kapral, R. *Phys. Rev. E* **1994**, *50*, 3560.
(28) Mikhailov, A.; Ertl, G. *Chem. Phys. Lett.* **1995**, *238*, 104. This equation without adsorption and desorption terms has been later derived in the theory of phase segregation in binary alloys: Giacomin, G.; Lebowitz, J. L. *Phys. Rev. Lett.* **1996**, *76*, 1094.
(29) Hill, T. L. *Statistical Mechanics*; McGraw-Hill: New York, 1956.
(30) (a) In the earlier paper[28] a discontinuous solution for the standing interface was derived by using in the bistable region the diffusion equation 17 without the additional term with the fourth-order derivative. Though this solution is formally correct, it is not stable in the framework of the full kinetic equation and therefore should be discarded. As has been brought to our attention by V. Zhdanov,[30b] the usual thermodynamical Maxwell condition 25 must determine in the considered case the curve of stationary coexistence of two phases. (b) V. P. Zhdanov, private communication.
(31) Bray, A. J. *Adv. Phys.* **1994**, *43*, 357.
(32) Lifshitz, E. M.; Pitaevskii, L. P. *Physical Kinetics*; Pergamon Press: Oxford, 1981.

JP961668W